



Design, modeling and control of a hybrid machine system

P.R. Ouyang ^a, Q. Li ^b, W.J. Zhang ^{a,*}, L.S. Guo ^c

^a *Advanced Engineering Design Laboratory, Department of Mechanical Engineering,
University of Saskatchewan, 57 Campus Drive, Saskatoon, SK S7N 5A9, Canada*

^b *School of Mechanical and Production Engineering, Nanyang Technological University, Singapore*

^c *Department of Agricultural Engineering, University of Illinois at Urbana-Champaign, 1304 W Penn Ave.,
Urbana, IL 61801, USA*

Received 15 January 2004; accepted 7 June 2004

Abstract

A hybrid machine is such a machine where its drive system integrates two types of motors: the servomotor and the constant velocity (CV) motor. The existing research on the hybrid machine prototypes usually uses two servomotors, of which one “mimic” the CV motor by prescribing a constant velocity trajectory profile. It is obvious that this departs away from the real situation where a CV motor is in place. The CV motor will bring in the velocity fluctuation which can not be attenuated by the CV motor itself due to the lack of a control mechanism in the CV motor, yet be propagated to the servomotor, and further to the end-effector of the machine. The general strategy for controlling the hybrid machine is therefore to model this propagated fluctuation and incorporate it into a controller for the servomotor. A controller based on the sliding mode control technique is proposed for the hybrid machine in this paper. The stability analysis shows that the controller is asymptotically stable. Simulation with a preliminary test demonstrates the effectiveness and robustness of this controller. Finally, we examine further performance improvement through attaching a flywheel on the CV motor to demonstrate the effectiveness of the synergy of the integration of mechanical and electrical means.

© 2004 Elsevier Ltd. All rights reserved.

* Corresponding author. Tel.: +1 306 966 5478; fax: +1 306 966 5427.
E-mail address: chris_zhang@enr.usask.ca (W.J. Zhang).

Keywords: Hybrid machine; Five-bar mechanism; Design; Dynamic model; Control; Trajectory tracking

1. Introduction

One of the features of intelligent production machines is its application flexibility. This feature can be obtained by using servomotors instead of constant velocity (CV) motors, as the servomotors are real-time controllable and off-line programmable. However, for all but very basic rotary motions, even this servo drive concept needs a transforming mechanism, such as a lead screw or a rack and pinion, or a coupler and slider to complement motion generation or to reach a required working position. The motions that have extreme acceleration characteristics can put severe torque requirements for the motor, while excessive torque fluctuations are likely to produce substantial heat in the motor windings. Also, the range and speed of obtainable output motions, using the servo drive concept, may be limited by certain motor characteristics, such as the motor's rated torque, peak power capability, and bandwidth. In the direct generation of alternating types of non-uniform motions, these servomotors have to provide the required current to produce an accelerating and a decelerating torque. This involves an energy interchange between the mechanical and electrical components, which may be difficult in realization, or the implementation may prove to be very inefficient.

On the other hand, for most manufacturing automation applications in high volume production industries, expensive multi-axis robots are employed for simple repetitive operations that require only a limited flexibility and their inherent flexibility is often underutilized. In order to provide a middle ground between conventional inflexible machines and overly flexible robots and to take the advantages of both the traditional mechanisms (which imply a closed chain mechanism) and the servo drivers, the association of a servomotor to a conventional mechanism has been studied. Tokuz [1,2] proposed the hybrid machine system concept and described modeling of an experimental setup for a hybrid machine. In his hybrid machine, a two-DOF epicyclical differential gearbox generates output motion that further drives a slider-crank mechanism. It should be noted that in his hybrid machine, the CV motor was physically substituted by a servomotor. The study showed that the required servomotor power to realize some predefined changes to the slider motion turns out to be smaller for this hybrid configuration than the "servo configuration". Herman et al. [3] used Tokuz's configuration to drive a cam mechanism, instead of a crank-slider mechanism, which was called a hybrid cam mechanism. They assumed that the CV motor has a large inertia to ensure its constant velocity. Through simulation, they showed that judicious selection of cam profiles, together with the hybrid machine concept, could lead to the reduction of peak torque and power in the servomotor up to 50%.

Greenough et al. [4] defined a hybrid machine as the machine consisting of a servomotor and a CV motor that are coupled through a two-DOF mechanism and drive a single output. The machine, which they presented, consists of a servomotor, a CV motor, a flywheel, a two-DOF mechanism and an output load. The servomotor

and CV motor drive two independent shafts of the mechanism. The flywheel is attached to the shaft of the CV motor. The CV motor provides the majority of the power to the member via the two-DOF mechanism, whilst the servomotor acts as a low torque-modulating device. They showed that the reduction of the power in the servomotor could be up to 70% of the power if the two servomotors are used. Their work did not consider trajectory tracking, and therefore, the torque (thus the power) was not computed from the dynamic model and the control law. Furthermore, due to the introduction of a flywheel on the CV motor, they ignored the speed fluctuation in the CV motor.

As implied in the above discussion, the control of a hybrid machine system is still a challenge problem. This is mainly because of: (1) the uncontrollability of the CV motor during the operation of the system, (2) the coupling of the dynamics between the two input links associated with the CV motor and the servomotor, respectively. A preliminary study we conducted shows that traditional PID and CTC control methods do not work well for the hybrid machine problem. The present study aimed to develop an understanding of the dynamic behavior of the hybrid machine that consists of the CV motor (not any substituted one by the servomotor) and the servomotor. We considered mainly two aspects of dynamic behavior: trajectory tracking and peak torque in the servomotor. A controller based on the sliding mode control technique [14–16] was developed to implement a general control strategy, i.e., designing the controller for servomotor to compensate the disturbance propagated from the CV motor due to its velocity fluctuation. Both the simulation and preliminary experimental studies were carried out to achieve this goal. The main task for the simulation study was to verify the developed controller. The velocity fluctuation in the CV motor was examined, and its impact to the dynamic performances in the servomotor was observed. Furthermore, the effect of the mechanical flywheel on the dynamic performances in the servomotor was studied, which is interesting because an optimal integration of mechanical design (it means for the design of a flywheel) and control system design can be observed—known as a mechatronic design approach [5,6].

This paper is organized as follows. Section 2 discusses the design of the hybrid machine system, including the mobility and workspace analysis, the selection of parameters, and hardware of the hybrid machine prototype. Section 3 discusses the dynamic model of the hybrid machine system where the dynamic model of the motors is also included. Section 4 develops a new control algorithm and presents a stability analysis for the algorithm in the case of trajectory tracking task. Section 5 presents the results of both the simulation and preliminary experimental studies. Section 6 is a conclusion.

2. Design of the hybrid machine system

2.1. Mobility of the hybrid machine system

Due to the uncontrollability of the CV motor, the full rotation of the link associated with the CV motor in the hybrid machine system (HMS for short) is a necessary

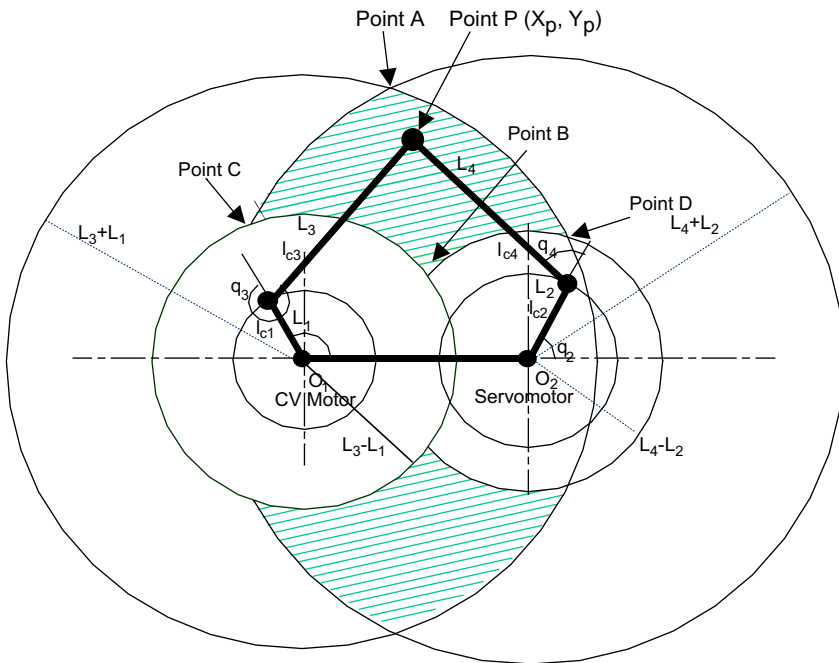


Fig. 1. Scheme of the HMS and its workspace.

condition. Therefore, the mobility analysis of the HMS is very important in order to fulfil its function. Mobility of the HMS is defined such that the two input links operate as an independent driving unit and are capable of revolving around their rotating shafts, respectively. Also, the linkage must be ensured that there is no singularity in the whole domain of the two input variables. In the following we derive the condition equations for the geometry of the linkage to ensure the mobility of the HMS. Fig. 1 shows the scheme of a five-bar linkage HMS. The angle between any two adjacent links of the linkage is defined as a revolvable angle if they can revolve relative to each other about the joint axis between them; otherwise the angle is a non-revolvable one. Except for the angle between two coupler links (end effector point P lies in the joint point of the two coupler links), all the other angles about their joints must be revolvable.

A theorem for the full rotatability of a closed loop linkage was given in [7,8]. For the HMS that is a five-bar linkage, the theorem can be described as follows.

2.1.1. Conditions

(1) The inequality equation

$$L_{\max} + L_{\min 2} + L_{\min 1} \leq L_m + L_n \tag{1}$$

where L_{\max} , $L_{\min 1}$ and $L_{\min 2}$ are the lengths of the longest link and the two shortest links of a five-bar linkage, L_m and L_n are the lengths of the other two links, and $L_{\max} \geq L_m \geq L_n \geq L_{\min 2} \geq L_{\min 1}$.

(2) In the two coupler links, one must be among (L_{\max}, L_m, L_n) .

2.1.2. Conclusion

The links with $L_{\min 1}$ and $L_{\min 2}$ may revolve relative to any of their neighbouring link, whereas any angle with two of the three other links (L_{\max}, L_m, L_n) is a non-revolvable one. This further implies that for each driver and its associated links one of them must be either $L_{\min 1}$ or $L_{\min 2}$.

In the case of the five-bar linkage HMS, we set the link which is common associated with two drivers, respectively, to be fixed one (frame or ground link), while $L_{\min 1}$ and $L_{\min 2}$ to be one of the other link associated with the driver 1 and the driver 2, respectively. According to the theorem above, the five-bar HMS is a double crank system.

2.2. Workspace analysis of the hybrid machine system

Workspace analysis has two objectives: (1) to determine the valid space for the end-effector to reach given the structure of a hybrid machine system, and (2) to determine the geometry of a hybrid machine system (e.g., the length of links) such that a desired trajectory is within the workspace. In both cases we need to find the relationship between the workspace and the geometry of the system.

As shown in Fig. 1, we set up the end-effector point P on the joint point of links 3 and 4. As the two motors which drive two input links respectively have full rotation property, we can consider that the linkage is composed of two dyads (links 1 and 3 and links 2 and 4). Therefore, the workspace of the five-bar linkage is the space common to the two-dyad workspace, i.e., the shadow region in Fig. 1.

From the above discussion one can see that the end-effector point P is on the boundary of the workspace when the angle between links 1 and 3 or between links 2 and 4 is 0 or π , respectively; in the both cases we obtain two sets of concentric circular arcs with their centres being at the two fixed joints, respectively. It is further noted that points A, B, C and D each corresponds to a situation where two links, one input link and the other coupler link, move to be a straight line, either in a folding or in an extending form. Let us call these particular situations the limit positions of the linkage. At the limit positions, end-effector P will reach a corner point or cusp, A, B, C or D.

2.3. Prototype of the hybrid machine system

A prototype of the HMS is shown in Fig. 2. The schematic diagram of the HMS is illustrated in Fig. 3. The HMS prototype consists of a five-bar linkage, an AC brushless servomotor and a servo amplifier with a gear transmission, an AC CV motor and a frequency controller, a shift encoder with resolution of 2000 ppr, a belt, and a

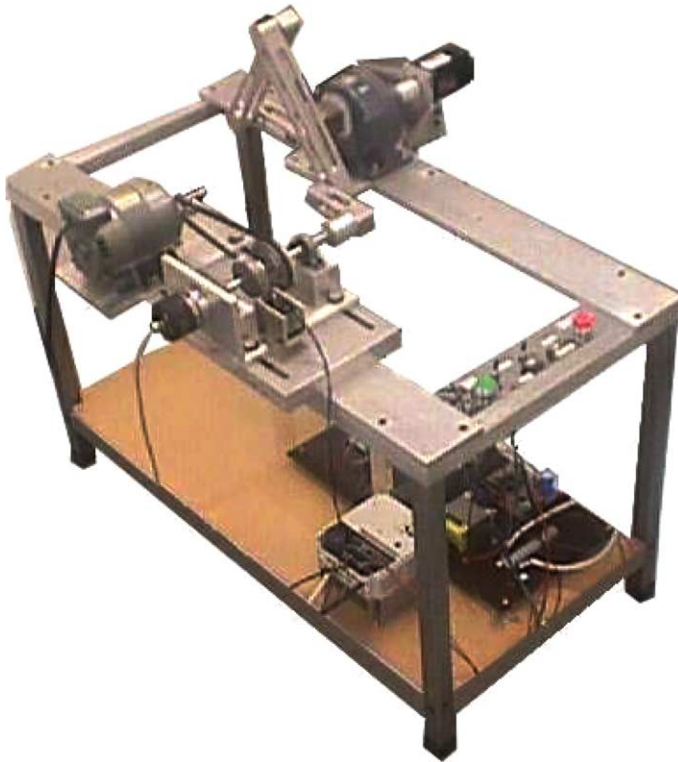


Fig. 2. A prototype of the hybrid machine system.

flywheel. In this arrangement, the AC CV motor with a belt of 3:1 and the servomotor generate, through a five-bar linkage, the expected output trajectories of the end-effector. Different combinations of motion profiles of the two inputs driven, respectively, by the AC CV motor and the AC servomotor can be implemented to obtain various types of output trajectories of the end-effector.

Hardware specifications of the control system are as follows:

- (1) Intel Pentium II 400 MHz Microcomputer with 64 MB RAM;
- (2) Programmable 14-bit AD/DA sampling card;
- (3) Programmable 8255 I/O card;
- (4) Incremental encoder brushless servomotor (SANYO DENKI, P30B06020-DXS00, 200 W, 3000 rpm) with servo amplifier (PUOA015EN41P00);
- (5) AC motor (SD18+, 190 W, 2800 rpm) with a frequency controller (FR-A024-S0.4K-EC, 220–240 V, 0.2–400 Hz, Sinusoidal PWM control system);
- (6) Incremental encoder (2000 ppr);
- (7) Synchronous up/down counter.

Physical parameters of the HMS are listed in [Table 1](#).

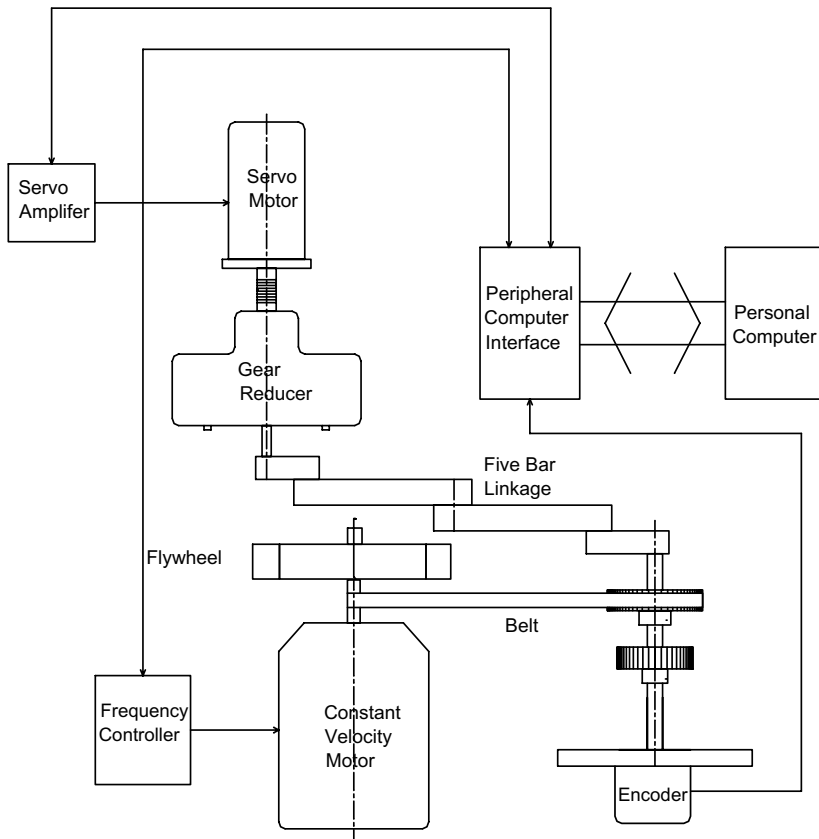


Fig. 3. Schematic diagram of the hybrid machine system.

Table 1
Physical parameters of the hybrid machine

Link i	m_i (kg)	L_i (m)	l_{ci} (m)	$I_i (\times 10^{-2} \text{kg m}^2)$
1	0.91	0.080	0.0061538	0.84718
2	0.28	0.100	0.02860	0.63001
3	0.38	0.250	0.125	4.00195
4	0.38	0.250	0.125	4.00195
5	–	0.250	–	–

3. Modelling of the HMS

Modelling of the dynamics of a plant is a key to effective control of the plant. The HMS prototype has two degrees of freedom, but only one is controllable. It is

necessary to build a complete dynamic model in such a way that the speed fluctuation in the CV motor can be compensated by a designed controller for the servomotor. In this section, both the dynamic model of the mechanical system and that of the motors are established and then integrated.

3.1. The dynamic model of the mechanical system

To derive the dynamic model of the hybrid machine, the method called the reduced model method for the closed chain mechanism in references [9,10] is employed in our study. As defined in Fig. 1, m_i, l_{ci}, L_i are, respectively, the mass, the distance to the center of mass from the joint of link i , and the length of link i , and I_i is the inertia of link i . For the more general application, we assume the center of mass of each link is off-line with an angle δ_i . Following the procedures in references [9,10], we can derive the dynamic model of the closed chain linkage as follows:

$$\begin{cases} D(q')\ddot{q}' + C(q', \dot{q}')\dot{q}' + g(q') = \tau \\ \dot{q}' = \rho(q')\dot{q} \\ q' = \sigma(q) \end{cases} \tag{2}$$

where

$$q = [q_1 \quad q_2]^T, \quad q' = [q_1 \quad q_2 \quad q_3 \quad q_4]^T$$

$$\dot{q} = [\dot{q}_1 \quad \dot{q}_2]^T, \quad \dot{q}' = [\dot{q}_1 \quad \dot{q}_2 \quad \dot{q}_3 \quad \dot{q}_4]^T$$

$$D(q') = \rho(q')^T D'(q) \rho(q') \tag{3}$$

$$C(q', \dot{q}') = \rho(q')^T C'(q', \dot{q}') \rho(q') + \rho(q')^T D'(q) \dot{\rho}(q', \dot{q}') \tag{4}$$

$$g(q') = \rho(q')^T g'(q') \tag{5}$$

$D'(q'), C'(q', \dot{q}'), g'(q'), \dot{\rho}(q', \dot{q}'), \rho(q')$, and $\sigma(q)$ are determined as follows.

By means of the Lagrangian method [11] we can obtain

$$D'(q') = \begin{bmatrix} d_{1,1} & 0 & d_{1,3} & 0 \\ 0 & d_{2,2} & 0 & d_{2,4} \\ d_{3,1} & 0 & d_{3,3} & 0 \\ 0 & d_{4,2} & 0 & d_{4,4} \end{bmatrix} \tag{6}$$

where

$$\begin{aligned}
 d_{1,1} &= m_1 l_{c1}^2 + m_3(L_1^2 + l_{c3}^2 + 2L_1 l_{c3} \cos(q_3 + \delta_3)) + I_1 + I_3 \\
 d_{1,3} &= m_3(l_{c3}^2 + L_1 l_{c3} \cos(q_3 + \delta_3)) + I_3, \\
 d_{2,2} &= m_2 l_{c2}^2 + m_4(L_2^2 + l_{c4}^2 + 2L_2 l_{c4} \cos(q_4 + \delta_4)) + I_2 + I_4, \\
 d_{2,4} &= m_4(l_{c4}^2 + L_2 l_{c4} \cos(q_4 + \delta_4)) + I_4, \quad d_{3,1} = d_{1,3} \\
 d_{3,3} &= m_3 l_{c3}^2 + I_3, \quad d_{4,2} = d_{2,4}, \quad d_{4,4} = m_4 l_{c4}^2 + I_4
 \end{aligned}$$

$$C'(q', \dot{q}') = \begin{bmatrix} h_1 \dot{q}_3 & 0 & h_1(\dot{q}_1 + \dot{q}_3) & 0 \\ 0 & h_2 \dot{q}_4 & 0 & h_2(\dot{q}_2 + \dot{q}_4) \\ -h_1 \dot{q}_1 & 0 & 0 & 0 \\ 0 & -h_2 \dot{q}_2 & 0 & 0 \end{bmatrix} \tag{7}$$

where $h_1 = -m_3 L_1 l_{c3} \sin(q_3)$, and $h_2 = -m_4 L_2 l_{c4} \sin(q_4)$,

$$g'(q') = g \begin{bmatrix} (m_1 l_{c1} + m_3 L_1) \cos(q_1 + \delta_1) + m_3 l_{c3} \cos(q_1 + q_3 + \delta_3) \\ (m_2 l_{c2} + m_4 L_2) \cos(q_2 + \delta_2) + m_4 l_{c4} \cos(q_2 + q_4 + \delta_4) \\ m_3 l_{c3} \cos(q_1 + q_3 + \delta_3) \\ m_4 l_{c4} \cos(q_2 + q_4 + \delta_4) \end{bmatrix} \tag{8}$$

where g is the gravitational acceleration constant.

$\dot{\rho}(q', \dot{q}')$, $\rho(q')$, and $\sigma(q)$ are further determined as follows.

The five-bar linkage is configured from two open-chain serial links by means of the introduction of two independent scleronomic holonomic constraint equations:

$$\phi(q') = \begin{bmatrix} \phi(1) \\ \phi(2) \end{bmatrix} = 0 \tag{9}$$

where

$$\phi(1) = L_1 \cos(q_1) + L_3 \cos(q_1 + q_3) - L_5 - L_2 \cos(q_2) - L_4 \cos(q_2 + q_4)$$

$$\phi(2) = L_1 \sin(q_1) + L_3 \sin(q_1 + q_3) - L_2 \sin(q_2) - L_4 \sin(q_2 + q_4)$$

The parameterization $\alpha(q') = q$ presents a transformation from $q' = [q_1 \ q_2 \ q_3 \ q_4]^T$ to $q = [q_1 \ q_2]^T$ and is given by

$$\alpha(q') = \begin{bmatrix} 1 & 0 & 0 & 0 \\ 0 & 1 & 0 & 0 \end{bmatrix} q' = q \tag{10}$$

Define

$$\psi(q') \triangleq \begin{bmatrix} \phi(q') \\ \alpha(q') \end{bmatrix}, \quad \psi_{q'}(q') \triangleq \frac{\partial \psi}{\partial q'}$$

Differentiating (9) with respect to q' and noticing (10) lead to

$$\psi_{q'}(q') = \begin{bmatrix} \psi_{q'}(1, 1) & \psi_{q'}(1, 2) & \psi_{q'}(1, 3) & \psi_{q'}(1, 4) \\ \psi_{q'}(2, 1) & \psi_{q'}(2, 2) & \psi_{q'}(2, 3) & \psi_{q'}(2, 4) \\ 1 & 0 & 0 & 0 \\ 0 & 1 & 0 & 0 \end{bmatrix} \tag{11}$$

where

$$\begin{aligned} \psi_{q'}(1, 1) &= -L_1 \sin(q_1) - L_3 \sin(q_1 + q_3), \\ \psi_{q'}(1, 2) &= L_2 \sin(q_2) + L_4 \sin(q_2 + q_4), \\ \psi_{q'}(1, 3) &= -L_3 \sin(q_1 + q_3), \quad \psi_{q'}(1, 4) = L_4 \sin(q_2 + q_4), \\ \psi_{q'}(2, 1) &= L_1 \cos(q_1) + L_3 \cos(q_1 + q_3), \\ \psi_{q'}(2, 2) &= -L_2 \cos(q_2) - L_4 \cos(q_2 + q_4), \\ \psi_{q'}(2, 3) &= L_3 \cos(q_1 + q_3), \quad \text{and} \quad \psi_{q'}(2, 4) = -L_4 \cos(q_2 + q_4) \end{aligned}$$

$\rho(q')$ can be expressed as follows:

$$\rho(q') = \psi_{q'}^{-1}(q') \begin{bmatrix} 0 & 0 \\ 0 & 0 \\ 1 & 0 \\ 0 & 1 \end{bmatrix} \tag{12}$$

$\det[\psi_{q'}(q')] \neq 0$, i.e. $\psi_{q'}^{-1}(q')$ exists if $q' = [q_1 \ q_2 \ q_3 \ q_4]^T$ is in the workspace region where the geometrical constraints are satisfied and the linkage is not in a singular configuration [9,10].

Since $\rho(q')$ is related to an inverse matrix, it is not easy to take the time derivative. But, the following expression for $\dot{\rho}(q', \dot{q}')$ can be obtained by pre-multiplying (11) with $\psi_{q'}(q')$ and taking the time derivative:

$$\dot{\rho}(q', \dot{q}') = -\psi_{q'}^{-1}(q') \dot{\psi}_{q'}(q', \dot{q}') \rho(q') \tag{13}$$

where $\dot{\psi}_{q'}(q', \dot{q}')$ can be obtained by differentiating (11) with respect to time.

In general, it is difficult to derive an analytic expression for the parameterisation $q' = \sigma(q)$, and it must be computed by means of numerical methods. For the closed-chain five-bar linkage, however, it is possible to do so; the following results can be obtained:

$$q_4 = 2 \tan^{-1} \left[\frac{\pm \sqrt{A(q_1, q_2)^2 + B(q_1, q_2)^2 - C(q_1, q_2)^2}}{C(q_1, q_2)} \right] + \tan^{-1} \left[\frac{B(q_1, q_2)}{A(q_1, q_2)} \right] - q_2 \tag{14}$$

$$q_3 = \tan^{-1} \left[\frac{\mu(q_1, q_2) + L_4 \sin(q_2 + q_4)}{\lambda(q_1, q_2) + L_4 \cos(q_2 + q_4)} \right] - q_1 \tag{15}$$

where

$$\begin{aligned} A(q_1, q_2) &= 2L_4\lambda(q_1, q_2), \quad B(q_1, q_2) = 2L_4\mu(q_1, q_2), \\ C(q_1, q_2) &= L_3^2 - L_4^2 - \lambda(q_1, q_2)^2 - \mu(q_1, q_2)^2, \\ \lambda(q_1, q_2) &= L_2 \cos(q_2) - L_1 \cos(q_1) + L_5, \quad \mu(q_1, q_2) = L_2 \sin(q_2) - L_1 \sin(q_1) \end{aligned}$$

3.2. The dynamic model of the motors

According to the HMS prototype as shown in Fig. 2, the torque applied on link 1 is produced by the AC constant velocity motor through a belt. The torque applied on link 2 is produced by the AC servomotor directly. Using the Newtonian kinematics law, the torque equation for the motor dynamics can be expressed by [12,13]

$$\tau_e = \tau_L + B_m\omega_r + J_m\dot{\omega}_r \quad (16)$$

where τ_e is the magnetic motor torque, B_m the viscous damping coefficient representing the torque loss, J_m the moment of inertia of the motor, τ_L the load torque, and ω_r the motor speed. Also, the motor torque can be expressed by

$$\tau_e = k_t i_q \quad (17)$$

Rearranging Eq. (16) leads to

$$\tau_e - \tau_L = B_m\omega_r + J_m\dot{\omega}_r \quad (18)$$

For the CV motor, the motor start-up is possible only if the electromagnetic torque τ_e is larger than the load torque τ_L . At the start-up, since the speed is zero and the left-hand side of (18) is greater than its right-hand side, the electric machine gets acceleration. As long as such a situation holds, the motor will continue to accelerate. The steady (work) state is reached when $\tau_e - \tau_L = B_m\omega_r$; at this point of time, the acceleration is zero and the motor operates at a constant speed.

Since the CV motor is not programmable, its electromagnetic torque is constant (so is its armature current) at its work state. If the load torque τ_L is constant, the constant speed motor will operate at a constant speed at all times. Unfortunately, in the process of the non-uniform periodical machine motion such as the hybrid machine, the load torque τ_L varies periodically, so the speed fluctuation will be present, even if the machine is driven by the constant speed motor. It should be noted that in the HMS, there is a belt between the CV motor and the link 1 of the five-bar linkage. So Equation (16) should be modified when the motor dynamics and the mechanical dynamics are integrated into a complete model, see discussion in the next section.

3.3. The integrated model of the HMS

In the arrangement of the hybrid machine as shown Fig. 1, the constant speed motor drives the actuated joint 1 through a belt with a ratio $\eta = 3$, while the servomotor drives directly the actuated joint 2. Therefore, we have $\omega_{r1} = \eta\dot{q}_1$ and $\omega_{r2} = \dot{q}_2$. Integration of the motor dynamic equation (18) and the HMS dynamic equation (2) to form a dynamic model of the full system is given as follows:

$$\begin{cases} \bar{D}(q')\ddot{q} + C(q', \dot{q}')\dot{q} + B\dot{q} + g(q') = \tau \\ \dot{q}' = \rho(q')\dot{q} \\ q' = \sigma(q) \end{cases} \quad (19)$$

where $\bar{D}(q') = (D(q') + J)$, $J = \text{diag}[\eta J_{m1} \ J_{m2}]$, $B = \text{diag}[\eta B_{m1} \ B_{m2}] \cdot J_{mi}$ and B_{mi} ($i = 1, 2$) are the moment of inertia and the viscous damping coefficient of the i th motor, respectively.

4. Control system design and stability analysis

4.1. Proposed control system

Sliding mode control (SMC) is a powerful control technique for nonlinear systems with uncertainty. The earliest notion of SMC strategy was proposed in the late 1960s [14], and a full survey can be found in [15]. The basic idea of sliding mode control is to constrain the state of the controlled system to reach a given manifold in the state-space and then to slide towards an equilibrium state along this manifold.

For the dynamic model in (19), the following properties and assumptions are held.

- (1) The inertia matrix $\bar{D}(q')$ is symmetric and positive definite.
- (2) $\bar{D}(q') - 2C(q', \dot{q}')$ is a skew symmetric matrix.
- (3) $\bar{D}(q')$, $C(q', \dot{q}')$ and $g(q')$ are bounded.
- (4) There exists uncertainty in the dynamic model. This means that $\bar{D}(q')$, $C(q', \dot{q}')$, and $g(q')$ are only partly known.

Properties 1 and 2 can be proved as follows.

The matrix $D(q')$ is symmetric and positive definite [9,10], and so is J . Therefore, the matrix $\bar{D}(q') = D(q') + J$ is symmetric and positive definite. Because the matrix J is constant, the term $\bar{D}(q') - 2C(q', \dot{q}') = \dot{D}(q') - 2C(q', \dot{q}')$ is skew [9,10].

The control objective is to drive the joint position q to the desired position q_d as close as possible with the presence of the speed fluctuation \dot{q}_1 on the CV motor. Define the tracking error as

$$\begin{cases} e = q - q_d \\ \dot{e} = \dot{q} - \dot{q}_d \end{cases} \quad (20)$$

where $q_d = [q_{1d} \ q_{2d}]^T$ and $\dot{q}_d = [\dot{q}_{1d} \ \dot{q}_{2d}]^T$. As link 1 is connected with a CV motor, for simplicity, we assume $\dot{q}_{1d} = \omega_d$, and $q_{1d} = \omega_{dt}$.

Define the sliding surface as

$$s = \dot{e} + \lambda e \quad (21)$$

where $\lambda = \text{diag}[\lambda_1, \lambda_2]$ in which λ_1 and λ_2 are positive constants.

Define the reference state as

$$\begin{cases} \dot{q}_r = \dot{q} - s = \dot{q}_d - \lambda e \\ \ddot{q}_r = \ddot{q} - \dot{s} = \ddot{q}_d - \lambda \dot{e} \end{cases} \quad (22)$$

Also let $\widehat{D}(q')$, $\widehat{C}(q', \dot{q}')$, and $\widehat{g}(q')$ be the estimations of $\overline{D}(q')$, $C(q', \dot{q}')$, and $g(q')$, respectively. Assume $\Delta\overline{D}(q') = \overline{D}(q') - \widehat{D}(q')$, $\Delta C(q', \dot{q}') = C(q', \dot{q}') - \widehat{C}(q', \dot{q}')$, and $\Delta g(q') = \widehat{g}(q') - g(q')$. Submitting Eqs. (20)–(22) into Eq. (19), the dynamic model of the hybrid mechanism in terms of the newly defined signal vector s can be derived as

$$\overline{D}(q')\dot{s} + C(q', \dot{q}')s + Bs = \begin{bmatrix} \tau_1 - f_1 + \Delta f_1 - B_{m1}\dot{q}_1 + B_{m1}s_1 \\ \tau_2 - f_2 + \Delta f_2 - B_{m2}\dot{q}_2 + B_{m2}s_2 \end{bmatrix} \quad (23)$$

where

$$f_1 = \widehat{d}_{11}(q')\ddot{q}_{r1} + \widehat{d}_{12}(q')\ddot{q}_{r2} + \widehat{c}_{11}(q', \dot{q}')\dot{q}_{r1} + \widehat{c}_{12}(q', \dot{q}')\dot{q}_{r2} + \widehat{g}_1(q') \quad (24)$$

$$f_2 = \widehat{d}_{21}(q')\ddot{q}_{r1} + \widehat{d}_{22}(q')\ddot{q}_{r2} + \widehat{c}_{21}(q', \dot{q}')\dot{q}_{r1} + \widehat{c}_{22}(q', \dot{q}')\dot{q}_{r2} + \widehat{g}_2(q') \quad (25)$$

$$\Delta f = [\Delta f_1 \quad \Delta f_2]^T = \Delta\overline{D}(q')\ddot{q}_r + \Delta C(q', \dot{q}')\dot{q}_r + \Delta g(q') \quad (26)$$

Assume that the torque in the CV motor is constant. When the CV motor is running at its operating speed, we assume that $\lambda_1 = 0$, and the constant torque for the CV motor is

$$\tau_1 = B_{m1}\omega_d \quad (27)$$

Further, the controlled torque for the servomotor is set as

$$\tau_2 = B_{m2}\dot{q}_{2r} + f_2 - k \operatorname{sgn}(s_2) - as_2 + \tau_r \quad (28)$$

where k is a design parameter that is a positive constant, τ_r is the designed torque of the servomotor to compensate the speed fluctuations in the CV motor. Assume $|\Delta f_i| < \Delta f_{bi}$, where Δf_{bi} is a positive constant that means the boundary of Δf_i . Choose k such that

$$k \geq \Delta f_{b2} \quad (29)$$

Choose the designed torque τ_r

$$\tau_r = \begin{cases} -|s_1|(|f_1| + \Delta f_{b1})/s_2, & \text{if } s_2 \neq 0 \\ 0, & \text{if } s_2 = 0 \end{cases} \quad (30)$$

The control system can be further represented by a block diagram, see Fig. 4. In Fig. 4 it is shown that the controller has three parts: (1) an estimated model; (2) a compensation of the speed fluctuation in the CV motor, and (3) a sliding mode control law.

After the above preparation, the stability of the controlled hybrid machine system can be concluded by the following theorem.

Theorem. For the HMS with uncertainty in the dynamic model (19), if the torque in the CV motor is given by (27), the controlled torque in the servomotor is given by (28), and the torque for the servomotor is defined as (30), then, the trajectory tracking errors $\dot{e}_1(t)$, $e_2(t)$, and $\dot{e}_2(t)$ will converge to zero when time t tends to infinite large, and $e_1(t)$

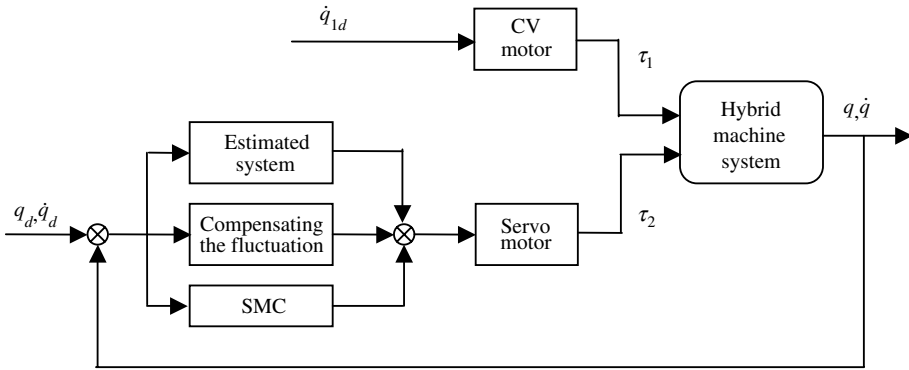


Fig. 4. Control diagram for the hybrid machine system.

is bounded for any time $t \geq 0$. The proof of this theorem will be provided in the next section.

4.2. Stability analysis

Proof. Submitting (27) and (28) into (23) yields

$$\bar{D}(q')\dot{s} + C(q', \dot{q}')s + \bar{B}s = \begin{bmatrix} -f_1 + \Delta f_1 \\ \tau_r + \Delta f_2 - k \operatorname{sgn}(s_2) \end{bmatrix} \tag{31}$$

where the matrix $\bar{B} = \operatorname{diag}[B_{m1} \ B_{m2} + a]$, and $a > 0$ is a design parameter. One can see that the matrix \bar{B} is symmetric and positive definite.

Now, consider the candidate Lyapunov function to be

$$V = \frac{1}{2}s^T \bar{D}(q')s \tag{32}$$

Since $\bar{D}(q')$ is symmetric and positive definite according to property 1, for $s \neq 0$ we have

$$V > 0 \tag{33}$$

Using property 2, it can be seen that

$$\begin{aligned} \dot{V} &= s^T \bar{D}(q')\dot{s} + \frac{1}{2}s^T \dot{\bar{D}}s(q') \\ &= s^T \left(\frac{1}{2}\dot{\bar{D}}(q') - C(q', \dot{q}') - \bar{B} \right) s + s^T \begin{bmatrix} -f_1 + \Delta f_1 \\ \tau_r + \Delta f_2 - k \operatorname{sgn}(s_2) \end{bmatrix} \\ &= -s^T \bar{B}s - s_1(f_1 + \Delta f_1) + s_2\tau_r + s_2(\Delta f_2 - k \operatorname{sgn}(s_2)) \end{aligned} \tag{34}$$

From (29), the following inequality holds:

$$s_2(\Delta f_2 - k \operatorname{sgn}(s_2)) \leq 0 \tag{35}$$

Using (30), it can easily be verified that

$$-s_1(f_1 + \Delta f_1) + s_2\tau_r = -s_1(f_1 + \Delta f_1) - |s_1|(|f_1| + \Delta f_{b1}) \leq 0 \tag{36}$$

As the matrix \bar{B} is symmetric and positive definite, we have

$$-s^T \bar{B} s \leq 0 \tag{37}$$

From (35)–(37), one can verify

$$\dot{V} \leq 0 \tag{38}$$

Eq. (32) can be viewed as an indicator of the energy of s . Therefore, Eq. (38) guarantees the decay of the energy of s as long as $s \neq 0$. According to the Lyapunov’s stability theorem, $s(t)$ will exponentially tends to zero when t tends to infinite large. From the standard stable filter theory, this implies that errors $\dot{e}_1(t)$, $e_2(t)$, and $\dot{e}_2(t)$ will exponentially converge to zero when time t tends to infinite large. Furthermore, since $\dot{e}_1(t)$ exponentially converge to zero, $e_1(t)$ will be normally bounded. \square

Several remarks are given further:

Remark 1. From (28), one can see that the controlled torque of the servomotor is discontinuous. In order to eliminate the chattering of the servomotor, the smoothing method introduced in [16] can be used as follows:

$$\tau_2 = B_{m2}\dot{q}_{2r} + f_2 - k \operatorname{sat}(s_2/\Phi) - as_2 + \tau_r \Phi > 0, \tag{39}$$

where Φ is called boundary layer.

Remark 2. As the sliding surface s is also discontinuous, so does the designed torque in (30). To avoid the chattering of the designed torque, Eq. (30) can be changed as

$$\tau_r = -\frac{|s_1|(|f_1| + \Delta f_{b1})s_2}{\delta + s_2^2} \tag{40}$$

where $\delta > 0$ is the boundary layer thickness.

Remark 3. After the smoothing method is used in (39) and (40) for the servomotor control, one can see that the trajectory tracking error is globally uniformly ultimately bounded, and the boundary can be controlled by carefully selected Φ and s .

5. Dynamic simulation of the HMS

In this section, simulation study is presented for the trajectory tracking of the desinged HMS prototype to examine the effectiveness of the proposed control

Table 2
The parameters of the two motors

Motor type	J (kgm ²)	B _m (Nms)
CV motor	0.5	0.5
Servomotor	0.05	0.05

algorithm. Also, the feasibility of attaching a flywheel to improve the tracking performance is studied. It should be noted that the uncertainty of the dynamic model is included in the simulation studies to give the feeling of robustness of the control system proposed.

The physical parameters of the HMS are drawn from the prototype shown in Fig. 2 and listed in Table 1, while the parameters of the two motors are recorded in Table 2.

5.1. Trajectory planning for the two input links

The desired trajectories for the two input links are expressed as one constant velocity rotation for the CV motor connecting with link 1 through a belt and the other Hermite polynomial of the fifth degree in t with continuous bounded conditions for position, velocity and acceleration for the servomotor driving link 2, that is,

$$q_1^d(t) = \omega_d t \quad (41)$$

$$q_2^d(t, t_f) = q_{20}^d + \left(6 \frac{t^5}{t_f^5} - 15 \frac{t^4}{t_f^4} + 10 \frac{t^3}{t_f^3} \right) (q_{2f}^d - q_{20}^d) \quad (42)$$

where $q_1^d(t)$ and $q_2^d(t, t_f)$ are the desired angular displacements for two input links, q_{20}^d and q_{2f}^d are the desired initial and final positions of the input link 2 driven by the servomotor, and t_f represents the time at which the desired trajectory for the end-effector reaches the desired final position. In the simulation, we assumed $\omega_d = 0.5\pi$ (rad/s), $q_{20}^d = 0$, $q_{2f}^d = 2\pi$, and $t_f = 4$ s. Also we let $q_1(0) = 0$, $q_2(0) = 0$ for simplification. Furthermore, the uncertainty of the dynamic model is estimated by applying factors to the corresponding parameters matrices as follows:

$$\widehat{D}(q') = 0.95\overline{D}(q'), \quad \widehat{C}(q', \dot{q}') = 0.9C(q', \dot{q}'), \quad \text{and} \quad \widehat{g}(q') = 1.05g(q')$$

The controlled torque for the servomotor is chosen as in (39), where $a = 10$, $\lambda_2 = 15$, and $k = 30$.

5.2. Trajectory tracking of the HMS

Simulation result is shown in Fig. 5. From Fig. 5, one can see that the maximum speed fluctuation in link 1 is about 0.1 rad/s that is about 6.4% of the desired speed, while the maximum position error is less than 0.06 rad. It is noted that a manual measurement of the velocity fluctuation on the CV motor through a tachometer confirmed the speed fluctuation. The high tracking performance (position error less

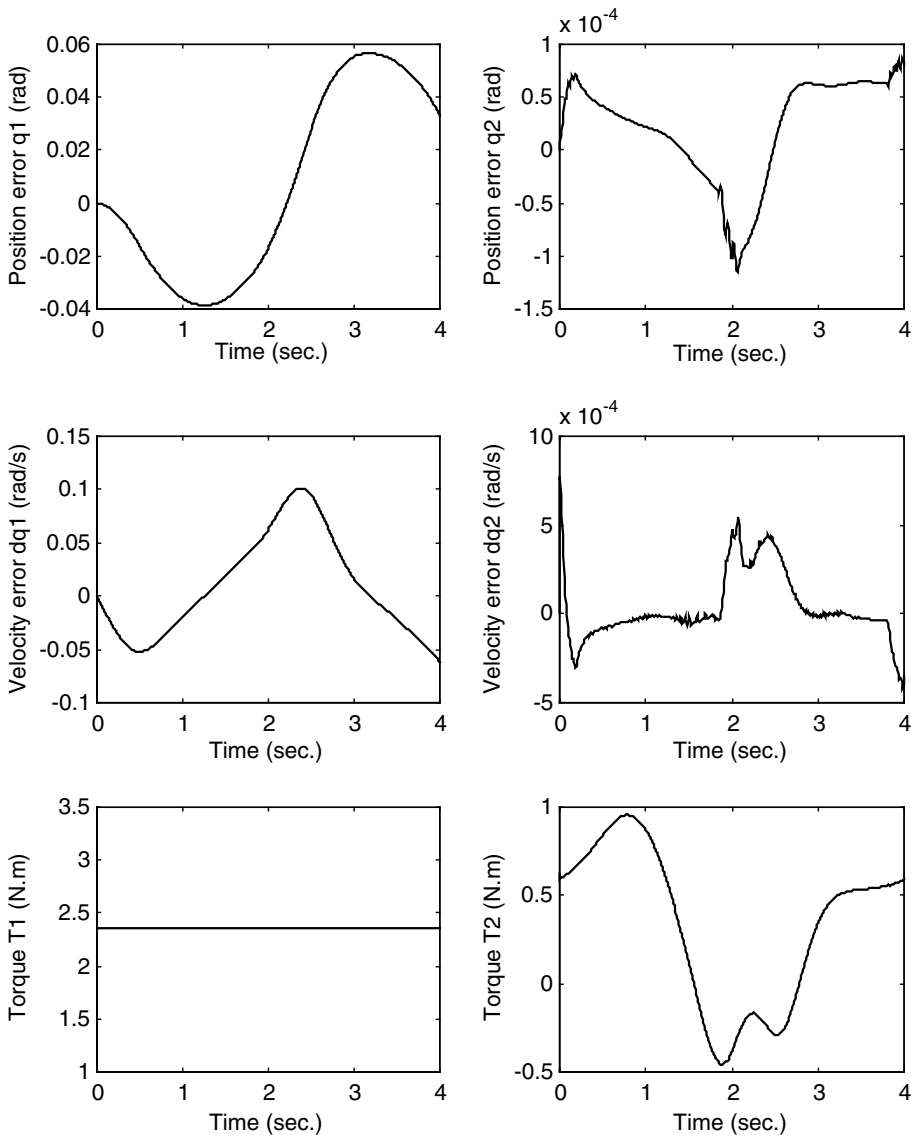


Fig. 5. Tracking performance for the HMS without flywheel.

than 10^{-4} rad, and velocity error less than 10^{-3} rad/s, respectively) for the servomotor was obtained. Furthermore, the controlled torque for the servomotor is smooth, which can avoid the chattering of the servomotor while the required torque for the CV motor is maintained at a constant level. The simulation result is promising.

5.3. Tracking performance improvement of the HMS by a flywheel

In mechanical design, it is common knowledge that adding a flywheel on the shaft of a CV motor can decrease the velocity fluctuation. To examine such an effect in the HMS, the flywheel inertia is included in the dynamic model. In the simulation, the same control parameters are chosen as above. Two flywheels with different inertias

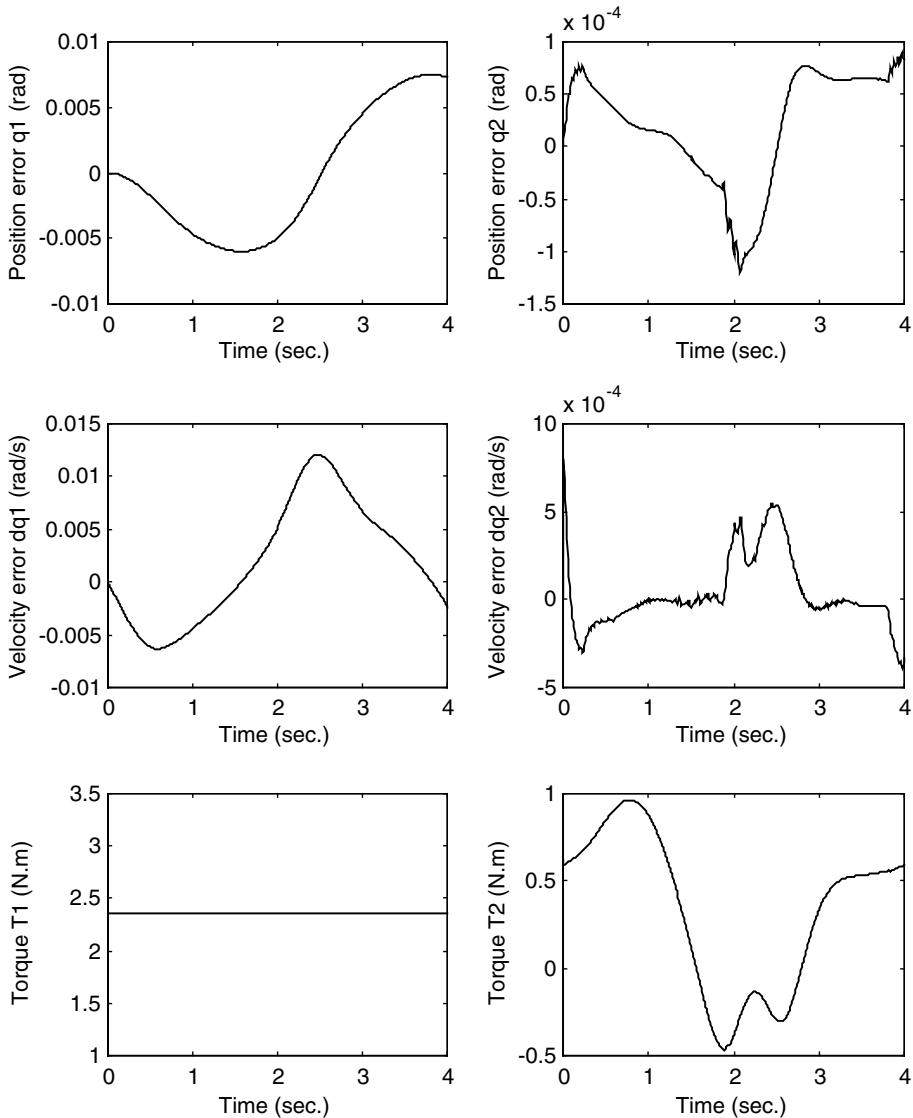


Fig. 6. Tracking performance for the HMS attaching a flywheel with $J_f = 5.0\text{kgm}^2$.

(5kgm^2 and 10kgm^2 , respectively) were used to examine their effects to the tracking performance and the required torque for the servomotor. Figs. 6 and 7 show the tracking performances after attaching a flywheel on the shaft of the CV motor.

It is observed that, by adding the flywheel, the overall tracking performance of the whole system is improved significantly, especially for link 1. The velocity fluctuation

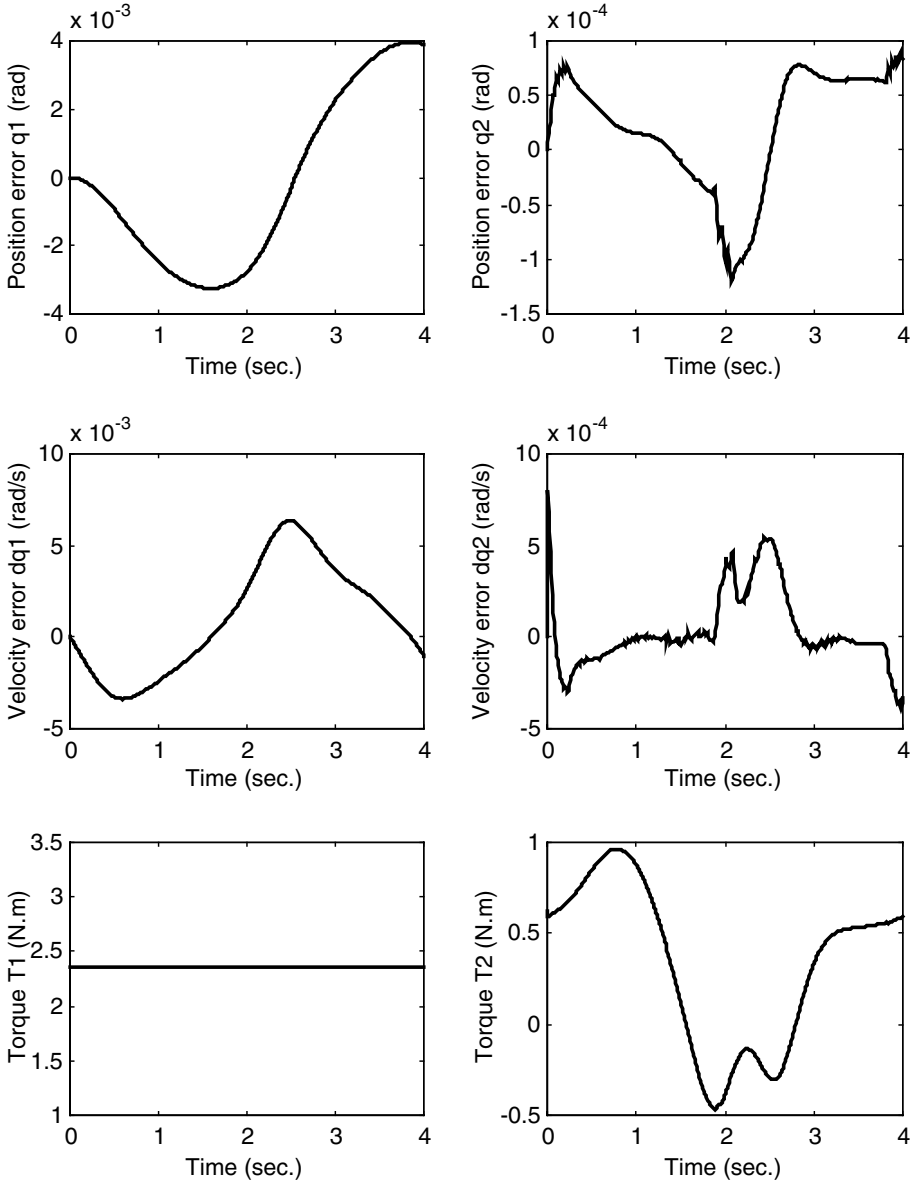


Fig. 7. Tracking performance for the HMS attaching a flywheel with $J_f = 10.0\text{kgm}^2$.

in the CV motor was reduced from 0.1 rad/s (no flywheel) to 0.012 rad/s (a small flywheel), and further to 0.006 rad/s (a big flywheel). Again, the reduction of the speed fluctuation in the CV motor was confirmed by the manual measurement using a tachometer. The maximum position error for link 1 was decreased from 0.06 rad to 0.01 rad, and to 0.004 rad, respectively. Also one can see that the tracking performance of the servomotor is still maintained at an excellent level, and the controlled torque is barely changed for these three cases. These results demonstrate the effectiveness and robustness of the control algorithm.

From Figs. 5–7, one can see that with the adding of the flywheel to the CV motor, the performance (the tracking errors) is improved considerably for the CV motor but not for the servomotor. This phenomenon is due to the special feature of the sliding mode control, i.e., the robustness of the SMC for the uncertainty of the dynamic model. The introduction of the flywheel can be viewed as “adding” some uncertainty in the dynamics of the HMS. As the control parameters for the servomotor remained the same for all three cases, the uncertain dynamics due to the flywheel may not change the performance of the controlled HMS.

6. Summary and conclusions

The hybrid machine system combines the advantages of the traditional machine and the servo driver technology in a way to provide a middle ground solution between the conventional inflexible machines and the overly flexible robots. However, the control of the HMS is a challenge due to the uncontrollability of the CV motor. In this paper, the design of the HMS was presented; the modelling of the full system including both the mechanical system and the driving system was discussed. A new control algorithm for the servomotor was proposed that can be used to compensate the speed fluctuation in the CV motor, and its stability was analyzed. Simulation studies for the trajectory tracking in the joint level have shown the effectiveness of this controller. The improvement of tracking performance with a mechanical flywheel added was demonstrated, which shows a great potential for system performance improvement by combining the mechanical principles and the electronic control principles in production systems development.

The limitation of the present work is its preliminary nature in the experiment, i.e., only the manual measurement of the speed fluctuation in the CV motor was performed, while this has provided some validation of the dynamic model derived. A more detailed experimental study is needed in the future.

Acknowledgment

This work is partially supported by the Natural Sciences and Engineering Research Council (NSERC) of Canada through a discovery grant to the third author.

References

- [1] Tokuz LC, Jones JR. Programmable modulation of motion using hybrid machines. *IMechE* 1991;C414/071:85–91.
- [2] Tokuz LC. Hybrid machine modeling and control. Phd dissertation, Liverpool Polytechnic, UK; 1992.
- [3] Straete HJ, Schutter JD. Hybrid cam mechanisms. *IEEE/ASME Transactions on Mechatronics* 1996;1(4):284–9.
- [4] Greenough JD et al. Design of hybrid machines. In: *Proceedings of the 9th IFTMM World Congress, Milan, Italy; 1995*. p. 2501–5.
- [5] Li Q, Zhang WJ, Chen L. Design for control (DFC): a concurrent engineering approach for mechatronic system design. *IEEE/ASME Trans Mechatron* 2001;6(2):161–9.
- [6] Zhang WJ, Li Q, Guo LS. Integrated design of mechanical structure and control algorithm for a programmable four-bar linkage. *IEEE/ASME Trans Mechatron* 1999;4(4):354–62.
- [7] Ting KL, Liu Y. Rotatability laws for N-bar kinematic chains and their proof. *Trans ASME J Mech Des* 1991;113(1):32–9.
- [8] Ting KL. Mobility criteria of single-loop N-bar linkage. *Trans ASME J Mech Des* 1991;111(4):504–7.
- [9] Ghorbel F, Gunawardana R. A validation study of PD control of a closed-chain mechanical system. In: *Proceedings of the 36th Conference on Decision and Control, San Diego, CA, USA; December 1997*. p. 1998–2004.
- [10] Ghorbel F. Modeling and PD control of a closed-chain mechanical system. In: *Proceedings of the 34th Conference on Decision and Control, New Orleans, LA, USA; December 1995*; p. 540–2.
- [11] Sciavicco L, Siciliano B. *Modeling and control of robot manipulators*. New York: The McGraw-Hill Companies, Inc.; 1996.
- [12] Nasar SA, Unnewehr LE. *Electromechanics and electric machines*. New York: John Wiley and Sons; 1979.
- [13] Pillay P, Krishnam R. Modeling, simulation and analysis of permanent-magnet motor drives. Part I: the permanent-magnet synchronous motor drive. *IEEE Trans Ind Appl* 1989;25(2):265–73.
- [14] Emelyanov SV. *Variable structure control systems*. Moscow: Nauka; 1967.
- [15] Utkin VI. *Variable structure systems with sliding modes*. *IEEE Trans Auto Contr* 1977;22(2):212–22.
- [16] Slotine JE, Li W. *Applied nonlinear control*. Englewood Cliffs, NJ: Prentice Hall; 1991.